arXiv:gr-qc/0310036v1 7 Oct 2003

The ST7 Interferometer

Robert Spero Andreas Kuhnert
Jet Propulsion Laboratory, California Institute of Technology

19 September, 2003

Abstract

Two homodyne Michelson interferferometers aboard the LISA Pathfinder spacecraft will measure the the positions of two free-floating test masses, as part of the NASA ST7 mission. The interferometer is required to measure the separation between the test masses with sensitivity of $30\,\mathrm{pm}/\sqrt{\mathrm{Hz}}$ at $10\,\mathrm{mHz}$. The readout scheme is described, error sources are analyzed, and experimental results are presented.

1 Introduction and Interferometer Description

The ST7 project is designed to demonstrate that test masses can be contained within a spacecraft, and left free from external disturbances at a level approximately 10 times higher than the nominal requirement for LISA [1] . The ST7 electrostatic system that contains, senses, and controls the test masses is designed to apply forces no larger than those that would lead to this displacement noise level, and the interferometer is designed to verify the absence of imposed force noise.

Dual homodyne Michelson interferometers (Figure 1) sense changes in the positions of the test masses. Centered on a common optical bench, there is one interferometer for each mass. The quantity of interest is z, the separation of test masses, which is equal to the sum of the two interferometer displacement outputs. The signal I_s is the total detected intensity for one interferometer; at the nominal operating point, I_s is half its maximum.

Changes in position of one of the test masses are detected as changes in the corresponding I_s.

Fluctuation in the orientation θ of the test mass is a source of error in the displacement readout. The signal I_d is the difference in intensity between two halves of the beam, as monitored by segmented photodiodes. I_d measures θ; it can be used to reduce the error either during data analysis, or in real-time by serving as the error-point in a control system.

As depicted in Figure 1, light a $1.06\,\mu$m wavelength NPRO laser enters on an optical fiber, and is collimated and converted to a free-space beam of approximately 1 mm diameter. The beam is split to feed two separate interferometers. The sum of the reference lengths (drawn vertically) is matched to the sum of the measurement lengths (drawn horizontally), to make the measurement of z insensitive to laser frequency. During data analysis, I_s and I_d are divided by the laser Intensity Monitor signal picked off before the interferometer, to form signals independent of the laser intensity.

This homodyne detection scheme has the advantage of simplicity: laser light is injected by a single fiber, there are no polarizers or modulators, and the displacement measurement is derived directly from the detected intensity. It requires that the masses be constrained to near the mid-fringe position, and that the detection electronics have low noise in the signal band of 1 mHz to 1 Hz. Calculations and measurements indicate that noise in the laser intensity and frequency and in the readout electronics are all sufficiently small to meet the ST7 performance requirements. A potential source of significant noise is fluctuation in θ giving a false reading of noise in z. We emphasize in this paper the mitigation of test mass orientation noise as sensed by the quadrant photodetectors.

2 Detected Signals and Angle Sensitivity

2.1 Total intensity

The intensity profile across the interfering beams at the photodetectors is determined by the addition of electric fields, E_1 from the reference mirror and E_2 from the test mass. The beams are like-polarized, and each has a Gaussian profile with radius w. The optical phase ϕ of E_2 is proportional to the position of the test mass. If E_2 is misaligned with respect to E_1 in the

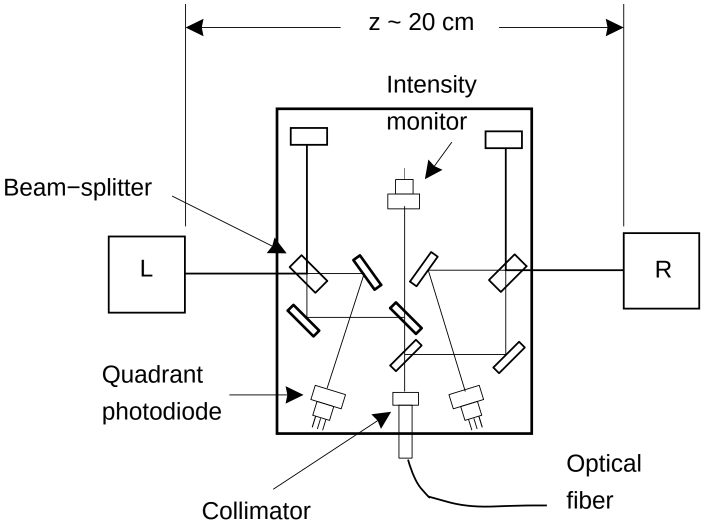

Figure 1: Schematic diagram of the ST7 interferometer. The distances to the L and R test masses are read out separately, and their separation is computed as the sum. The "sensitive path" bold lines indicate the distances measured by the interferometer.

x-direction by the slight angle θ,

$$\begin{aligned} E_1 &= e^{-r^2/w^2} && (1) \\ E_2 &= e^{i(\phi + kx\sin\theta) - r^2/w^2}, && (2) \end{aligned}$$

where the wavenumber k is related to the wavelength λ by $k = 2\pi/\lambda$. The resulting intensity at the plane of detection is

$$I(r,\psi) = |E_1 + E_2|^2 = 2e^{-2r^2/w^2}\left[1 + \cos(\phi + kx\sin\theta)\right], \tag{3}$$

where (r, ψ) are the polar coordinates of the intensity profile and $x = r\sin\psi$.

Integrating Equation 3 over all (r, ψ) and normalizing to unit maximum, the total intensity of the interference signal is

$$I_s = \frac{1 + \cos\phi\exp(-k^2w^2\theta^2/8)}{2}. \tag{4}$$

Equation 4 identifies the Visibility, V, defined as (max - min)/(max + min) of I_s, as $V(\theta) = \exp(-k^2w^2\theta^2/8)$, and

$$I_s = \frac{1}{2}\left(1 + V\cos\phi\right). \tag{5}$$

The sensitivity of I_s to alignment change is

$$\frac{dI_s}{d\theta} = -\frac{1}{8}k^2w^2\theta V\cos\phi \approx -\frac{1}{8}k^2w^2\theta\cos\phi\left(1 - \frac{1}{8}(kw\theta)^2\right), \tag{6}$$

where the expansion is valid for small misalignment θ.

2.2 Difference signal

Consider the division of the beam into upper ($0 < \psi < \pi$) and lower ($-\pi < \psi < 0$) halves:

$$I_{u,l} = \int_0^{\pi,-\pi} d\psi \int_0^{\infty} rdr\, I(r,\psi), = -\frac{1}{4}\left[1 + V\left(\cos\phi \pm \sin\phi\,\mathrm{erfi}(\sqrt{-\log V})\right)\right] \tag{7}$$

where erfi is the complex error function. Using the identity $\cos\phi + A\sin\phi = \cos(\phi - \phi_0)/\cos\phi_0$, with $\phi_0 = \arctan A$, the phase shift between I_u and I_l is

$$\Delta\phi = 2\arctan\left[\mathrm{erfi}\sqrt{-\log V}\right]. \tag{8}$$

V can be maximized by aligning the interferometer to minimize $\Delta\phi$.

The magnitude of the difference signal, $I_d = I_u - I_l$, also provides a measure of θ.

$$I_d = -\frac{V}{2}\sin\phi \; \mathrm{erfi}\left(\sqrt{-\log V}\right) = -\frac{V}{2}\sin\phi \; \mathrm{erfi}\left(kw\theta/\sqrt{8}\right) \tag{9}$$

I_s (Equation 5) and I_d are relatively shifted by $\pi/2$ with respect to ϕ. Taylor expanding Equation 9 for small θ:

$$I_d \approx -\frac{1}{\sqrt{8\pi}}k\theta w\sin\phi\left[1-\frac{1}{12}(k\theta w)^2\right] = -\frac{1}{\sqrt{8\pi}}k\theta w\sin\phi\left[1-\frac{2}{3}\log V\right] \tag{10}$$

The sensitivity of I_d to θ is

$$\frac{dI_d}{d\theta} = -\frac{1}{\sqrt{8\pi}}kw\sin\phi\left[1-\sqrt{\frac{\pi}{8}}Vkw\theta\;\mathrm{erfi}[kw\theta/\sqrt{8}]\right]. \tag{11}$$

Equation 11 has the Taylor expansion

$$\frac{dI_d}{d\theta} \approx -\frac{1}{\sqrt{8\pi}}kw\sin\phi\left[1-\left(\frac{kw\theta}{2}\right)^2\right] \approx -\frac{1}{\sqrt{8\pi}}kw\sin\phi\,[2V-1]. \tag{12}$$

2.3 Requirements on static alignment θ or alignment sensing

If the static misalignment θ were sufficiently small, the noise due to alignment fluctuations $\tilde{\theta}(f)$ could be negligible, and would need not be monitored. Since the error in position readout associated with offset ϕ from fringe center is $dz_\phi = d\phi/(2k)$,

$$\frac{dz_\phi}{d\theta} = \frac{1}{2k}\frac{d\phi}{d\theta} = \frac{1}{2k}\frac{dI_s/d\theta}{dI_s/d\phi} = \frac{dz_\phi}{d\theta} = \frac{1}{8}\frac{kw^2\theta}{\tan\phi}. \tag{13}$$

Let z_0 be the operating point deviation from fringe center $\phi = \pi/2$. Then $dz_\phi/d\theta = kw^2\theta\tan(2kz_0)/8$, implying the root Power Spectral Density (RPSD) in displacement noise $\tilde{z}(f)$ for angle-noise $\tilde{\theta}(f)$, fringe offset z_0, and alignment off-normal by θ is

$$\tilde{z}_\phi(f) = \frac{1}{8}\tilde{\theta}(f)\theta kw^2\tan(2kz_0). \tag{14}$$

For example, with $w = 0.5\,\mathrm{mm}$, $\tilde{\theta}(f) = 1\,\mu\mathrm{rad}/\sqrt{\mathrm{Hz}}$, static misalignment $\theta = 100\,\mu\mathrm{rad}$, and mass position offset $z_0 = 42\,\mathrm{nm}$, the noise contribution is $\tilde{z}(f) = 10\,\mathrm{pm}/\sqrt{\mathrm{Hz}}$.

While this error vanishes at the half-intensity point $z_0 = 0$, two other additive error terms are independent of z_0. If the interferometer beam strikes the test mass off-center by a distance h, then there is a "sine error" $dz_h/d\theta = (d/d\theta)(h \sin\theta) \approx h$. There is also a "cosine error" associated with the combination of wavefronts [3]. If the path from the test mass to the beam-splitter is p, the cosine error is $dz_p/d\theta = (d/d\theta)(p\cos\theta) \approx -p\theta$. Combining these terms with Equation 13, the sensitivity of position readout z to angle fluctuation θ is

$$\frac{dz}{d\theta} \approx h + \theta \left[\frac{kw^2}{8} \tan(2kz_0) - p \right]. \tag{15}$$

Note that the first and last terms can be cancelled by aligning θ or h to satisfy $h = p\theta$. For comparison, the response of a heterodyne interferometer such as that used in the LISA Test Package (LTP) ESA counterpart of ST7 [5] does not depend on z_0, and its θ-sensitivity is simply $dz/dh \approx h - p\theta$. Eliminating θ-sensitivity on ST7 requires either holding z_0 fixed, or measuring z_0 (inferred from I_s) and θ (inferred from I_d, Equation 9).

3 Experimental Results

Measurements were conducted on a laboratory test apparatus with dimensions similar to those of ST7—see Figure 2. The Reference mirrors and beam-splitters, made from ULE [2] glass, are optically contacted to a ULE plate. The plate is mounted on a stage that can be moved in z direction by a PZT actuator. Measurement mirrors in separate, conventional mounts stand in for the test masses. One of the measurement mirrors is mounted on a commercial [4] 3-piezo actuator to allow θ angle actuation. The spacing between the measurement mirrors is determined by a stainless steel mounting plate, and the apparatus is in an evacuated chamber.

Noise performance of the interferometers is shown in Figure 3. These data were collected six hours after the chamber was evacuated, to allow the temperature to stabilize. The Noise Allocation curve is the error budget allocation to the RPSD of $\tilde{z}(f)$. The noise levels for both the Left and Right interferometers are below this allocation level, including $< 30\,\mathrm{pm}/\sqrt{\mathrm{Hz}}$ at $10\,\mathrm{mHz}$. The peak at 20 mHz is due to intentional sinusoidal modulation of z, `st7-optical-bench-small.jpg`

Figure 2: Photograph of laboratory test interferometer.

to verify calibration and to measure the difference in the two interferometers' responses. The calibration peaks match to 0.5%. Also shown is the RPSD of the temperature in the vacuum chamber. Time-domain correlations are observed between the interferometer output and the temperature for times on the order of 10^4 sec and longer (not shown).

For the data shown in Figure 4, the interferometer was aligned for best visibility (minimum of I_s nearly zero, $V \approx 1$), and the optical bench was moved at constant velocity in the z direction while θ was modulated sinusoidally with amplitude $70\,\mu$rad p-p. Ignoring the fast θ response, the small phase shift $\Delta\phi$ between I_u and I_l corresponds to $V \approx 1$, in accordance with Equation 8.

Also in qualitative agreement with expectation is the response of the difference signal to modulation, Equation 11. At the half-intensity point, $\phi = \pi/2$, $dI_d/d\theta$ is expected to be maximum, corresponding to the maximum response to θ modulation in the experimental results. The observed sensitivity of the sum signal to θ, $dI_s/d\theta$ also agrees qualitatively with the predicted ϕ-dependence. Equation 6 says that $dI_s/d\theta$ should be maximum at the half-fringe, and the observed maxima are near the half-fringe points.

Figure 5 shows that when the beam is centered ($h \approx 0$), the difference response $dI_d/d\theta$ is much larger than the sum response $dI_s/d\theta$. That is, under

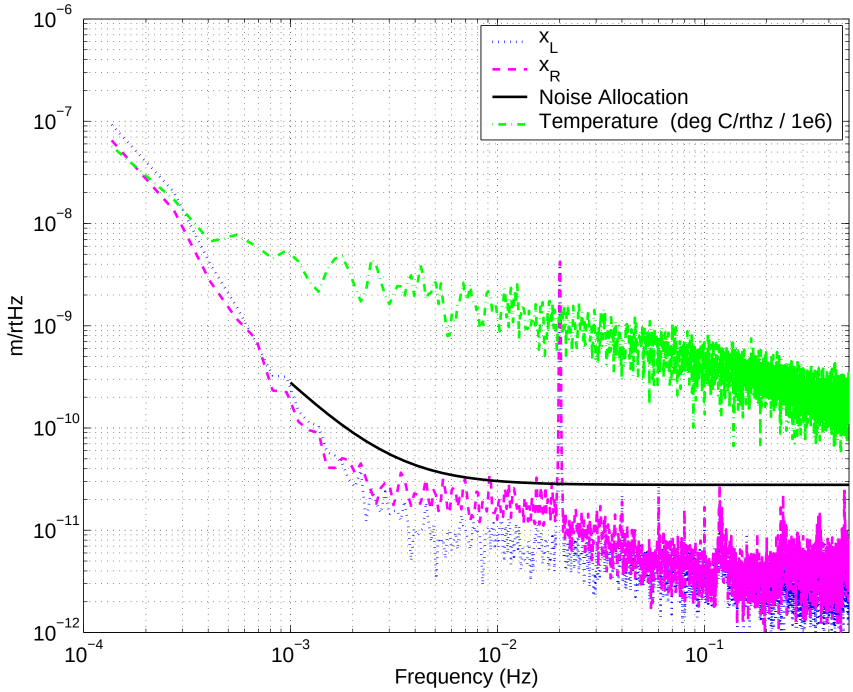

Figure 3: Noise spectra from the laboratory test interferometers, x_L and x_R measuring the left- and right-handed paths.

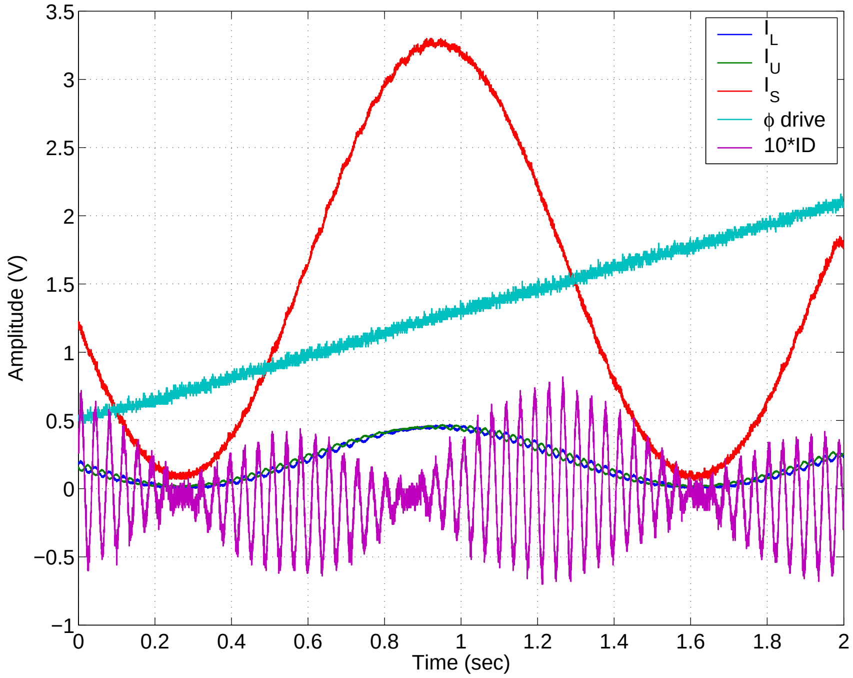

Figure 4: Intensity measurements with $V \approx 1$ alignment, z moved at constant velocity, and angular modulation $d\theta = 70\,\mu$rad p-p. The I_S trace is derived from a separate single-element photoreceiver.

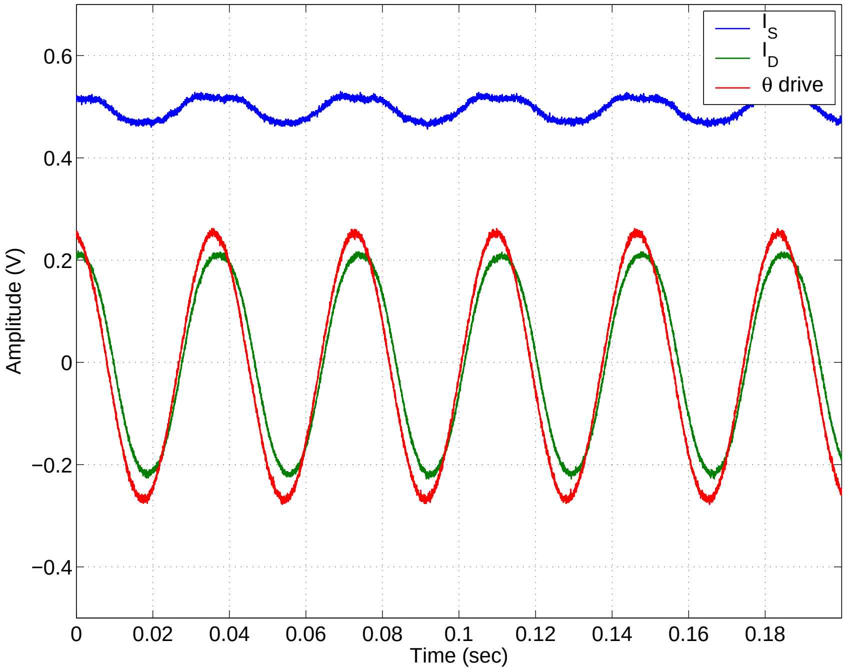

Figure 5: Longitudinal position z adjusted near the nominal half-intensity point, $\phi = \pi/2$. Transverse position h adjusted for minimum fluctuation in I_s. $d\theta = 350\,\mu$rad p-p.

nominal operating conditions, the diagnostic readout dI_d of the error source $d\theta$ is larger than its contribution to error in the signal, dI_s.

This research was performed at the Jet Propulsion Laboratory, California Institute of Technology, under a contract to the National Aeronautics and Space Administration.

References

References

[1] "Laser Interferometer Space Antenna: Pre-Phase A Report," 2nd ed, July 1998, available for public download from `ftp://ftp.ipp-garching.mpg.de/pub/grav/lisa/ppa2/ppa2.09.pdf`.

[2] A product of Corning Incorporated, Semiconductor Materials Business, Canton, New York, `http://www.corning.com/semiconductormaterials`

[3] Logan J. et. al. 2002 *Applied Optics* **41** 21

[4] A product of Physic Instrumente (PI) GmbH & Co. KG, Palmbach, Germany, `http://www.pi.ws`

[5] Vitale S., "The SMART-2 LISA Test Flight," and Heinzel, G. "The SMART-2 LTP IFO and Phasemeter," these Proceedings.

This figure "st7-optical-bench-small.jpg" is available in "jpg" format from:

http://arXiv.org/ps/gr-qc/0310036v1